Self-Concentration and Large-Scale Coherence in Bacterial Dynamics

Christopher Dombrowski,[1] Luis Cisneros,[1] Sunita Chatkaew,[1] Raymond E. Goldstein,[1,2] and John O. Kessler[1]

[1]*Department of Physics, University of Arizona, Tucson, Arizona 85721, USA*

[2]*Program in Applied Mathematics, University of Arizona, Tucson, Arizona 85721, USA*

(Received 23 December 2003; published 24 August 2004)

Suspensions of aerobic bacteria often develop flows from the interplay of chemotaxis and buoyancy. We find in sessile drops that flows related to those in the Boycott effect of sedimentation carry bioconvective plumes down the slanted meniscus and concentrate cells at the drop edge, while in pendant drops such self-concentration occurs at the bottom. On scales much larger than a cell, concentrated regions in both geometries exhibit transient, reconstituting, high-speed jets straddled by vortex streets. A mechanism for large-scale coherence is proposed based on hydrodynamic interactions between swimming cells.

DOI: 10.1103/PhysRevLett.93.098103 PACS numbers: 87.18.Ed, 05.65.+b, 47.20.–k, 47.54.+r

Bacterial chemotaxis, oriented swimming along chemical gradients, is generally viewed as locomotion in an otherwise quiescent fluid [1]. Yet, the very flagella which propel the cell inevitably stir up the fluid through their high-speed rotation, bundling, and unbundling. Conventional arguments [2] showing the irrelevance of advection compared to diffusion are based on the smallness of the Peclet number $\mathrm{Pe} = UL/D$. For a swimmer of micron scale L, moving at a speed U of several body lengths per second, and $D \sim 10^{-5}\ \mathrm{cm^2\,s^{-1}}$ a solute diffusion constant, we have $\mathrm{Pe} \sim 10^{-2}$, confirming this *for an isolated swimmer*. Yet, the collective hydrodynamics of concentrated assemblies of cells greatly changes this situation, yielding $\mathrm{Pe} > 1$. Such assemblies can arise due to the joint action of chemotaxis, a symmetry breaking source of metabolite(s), and gravity. Once concentrated, the collectively driven hydrodynamics globally outcompetes diffusion.

Here we report striking collective effects in bacterial suspensions in which strong microscale mixing arises from two related aspects of cellular swimming in fluid drops: *self-concentration* and *large-scale dynamic coherence*. The first arises from chemotactically generated accumulations of cells that encounter, then slide down a slanted meniscus, resulting in even higher concentrations (Figs. 1 and 2). Dynamic coherence develops within that nearly close packed population. It appears as jets and surges, straddled by vortices, often moving $>100\ \mu\mathrm{m/s}$, over scales $>100\ \mu\mathrm{m}$, yielding $\mathrm{Pe} \gtrsim 1$. These speeds and lengths exceed greatly the swimming speeds and size of the organisms. Ours are perhaps the first flow visualizations to provide information on the manner by which swimming bacteria may order. Although these patterns are different from ordering suggested by early theories [3–5] proposed to describe "flocking," they may provide evidence of an instability recently proposed [6,7]. Finally, we suggest links to quorum sensing [8] and biofilm formation [9].

Experiments were conducted on suspensions of strains 1085 and YB886 of *Bacillus subtilis*, a peritrichously flagellated rod-shaped bacterium $4 \times 0.7\ \mu\mathrm{m}$. Spores stored on agar or sand were used to inoculate nutrient medium [10]. Drops of suspension were studied on plastic or glass-bottomed petri dishes. To minimize evaporative flows that can advect suspended particles to the drop edge [11], high humidity in the closed chamber was maintained by additional fluid reservoirs. Control experiments with microspheres showed no evidence of such flows. Dark-field videos of macroscopic patterns were obtained with a digital camera (Hamamatsu C-7300) viewing light scattered by the sample. Bright-field objectives on inverted microscopes were used for higher magnifications. Particle tracking studies with commercial software (Motion Analysis Corp.) were also performed.

The consumption of dissolved oxygen by cells and its replenishment from the fluid-air interface sets the stage

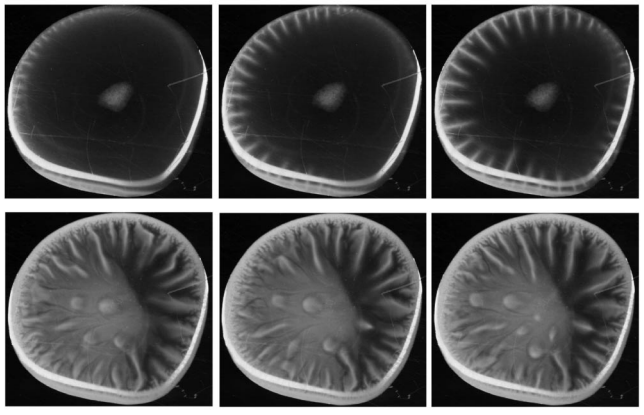

FIG. 1. Bioconvection in a sessile drop of diameter 1 cm. Top: images 5 min apart show the traveling-wave bio-Boycott convection that appears first at the drop edge. Bottom: images 2 min apart show self-concentration seen from above, beginning as vertical plumes which migrate outward.

for bioconvection. Bacteria consume $\sim 10^6$ oxygen molecules/sec [1]. At a typical cell concentration $n \sim 10^9$ cm^{-3} [12], the saturation oxygen concentration $c_s \sim 1.5 \times 10^{17}$ cm^{-3} is consumed within minutes [10], and the bacteria swim toward the surface, up the developing inward gradient of diffusing oxygen. A bacterium is about 10% denser than the fluid, so the buoyantly unstable surface accumulation of cells produces heavy, bacteria-rich plumes. With a horizontal meniscus, the plumes, rolls, and other complex bioconvection patterns take on a variety of forms much richer [10] than in the familiar thermal convection [13]. Figure 1(top) shows that in a sessile drop with slanting interface of center thickness $h \sim 2$ mm on glass, the first "plumes" are stripes perpendicular to the contact line [14]. They may travel along it, particularly if the meniscus curvature varies. As the cell density increases over time plumes of diameter $\sim$1 mm migrate outward at a velocity $\sim$0.01 cm/s [Fig. 1(bottom)]. They coexist with meniscus stripes for several hours then die down.

Viewing self-concentration from the side in Hele-Shaw geometry clarifies this process. Early in bioconvection, cells move toward the surface from a depletion region of thickness l [10,15] [Figs. 2(a)–2(c)]. The bottom of the depletion zone is marked by a very sharp boundary with the high cell concentration below. The cells remain in the latter region because the oxygen concentration is so low that their motility is greatly reduced (at least until large-scale mixing reintroduces oxygen). In our experiments, chemotactic migration of cells out of the depletion zone takes $\sim$100 s, consistent with traversal of a 0.1 cm layer with a typical chemotactic velocity $v_c \sim 10^{-3}$ cm/s. The thickness d of the ultimate layer of high concentration [Fig. 2(e)], can be estimated in a model of chemotaxis with $n_t = -\nabla \cdot \mathbf{j}$, where the flux $\mathbf{j} = -D_n \nabla + n\mathbf{v}_c$, and $D_n \sim 10^{-5}$ cm^2/s is the bacterial diffusion coefficient. In a quasisteady state there is an exponential profile on a scale $d \sim D_n/v_c \sim 0.01$ cm, small compared both to the plume width and depth of the drop, as in our observations. Figures 2(e) and 2(f) show that the surface layer breaks up into plumes that are pulled down the meniscus under gravity rather than penetrate fully through the bulk fluid.

Though more complex, this dynamic is akin to the Boycott effect in sedimentation [16], in which tilting a chamber produces along the upper slanted wall a depletion of particles and an upward current that entrains bulk fluid. Here, the sliding velocity of the layer arises from a balance between the gravitational force and drag from the subphase [17]; one finds $u \sim hd\Delta\rho g \sin(\theta)/\eta$ with θ the interfacial tangent angle. With $h \sim 0.2$ cm, $d \sim 0.01$ cm, $\Delta\rho \sim 0.10\phi \sim 0.001$ g/cm^3, $\eta = 0.01P$, and $\theta \simeq 0.1$, we find $u \sim 0.01$ cm/s, consistent with the observed velocity [18]. Flow along the slanting meniscus brings cells to the contact line and fluid recirculates toward the drop center, stirring up the region below the original depletion zone, but, *most cells remain trapped in the meniscus region.* Flow visualization indicates a vortex in the "nose" region [19], and it appears that entrainment in that flow augmented by high oxygen concentration near the meniscus trumps return advection as a transport mechanism.

In drops pendant from the ceiling of a closed chamber, oxygentaxis and sliding cooperate to bring cells to the lowest part, where they accumulate to high concentration in minutes, far faster than possible by gravitational sedimentation at the Stokes settling speed $\sim$0.2 μm/s. In self-concentrated regions of sessile and also pendant geometries, we find transient, reconstituting, coherent structures [10]. Figure 3 shows the turbulent appearance of the swimming near the contact line [20], where the volume fraction is $\gtrsim 0.1$. Lacking symmetry breaking by the contact line, patterns in pendant drops are more isotropic. These flows were analyzed with particle-imaging-velocimetry (PIV, Dantec), the bacteria acting both as flow generators and markers—the *cinemagraphic*

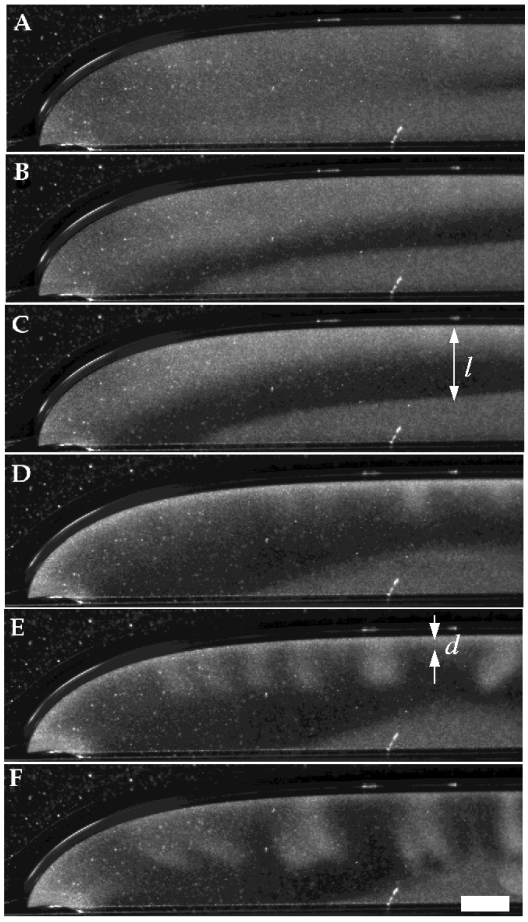

FIG. 2. Dark-field side views of self-concentrative flows between two coverslips spaced 1 mm apart: (a) uniform initial concentration; (b),(c) development of depletion layer as cells swim upward; (d)–(f) plumes carried to nose of drop, dragged by surface layer. Depletion and accumulation layer thicknesses l and d are shown. The scale bar is 1 mm.

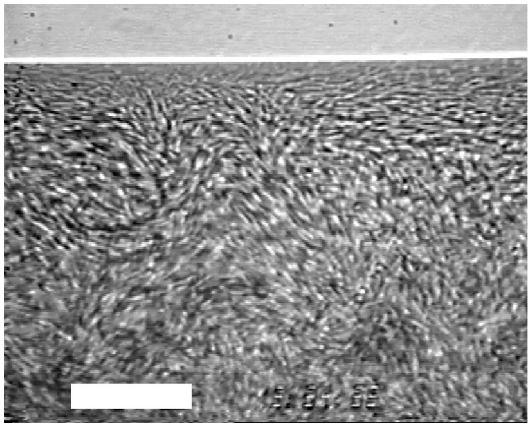

FIG. 3. Bacterial "turbulence" in a sessile drop, viewed from below through the bottom of a petri dish. Gravity is perpendicular to the plane of the picture, and the horizontal white line near the top is the air-water-plastic contact line. The central fuzziness is due to collective motion, not quite captured at the frame rate of 1/30 s. The scale bar is 35 μm.

mode. Such measurements are projections into the in-plane dimensions $\mathbf{x}_\parallel = (x, y)$ of three-dimensional patterns, albeit confined to thin layers. Figure 4 shows a typical velocity field $\mathbf{v}(\mathbf{x}_\parallel)$, with a meandering *jet* of high collective velocities (~ 50 μm/s) and surrounding *vortices*. The vortices nearest the leftward-directed jet flow clockwise above and counterclockwise below, as in a Kelvin-Helmholtz instability, or, anomalously at such low Reynolds numbers, a von Karman vortex street.

We have computed the velocity correlation $I(\mathbf{r}_\parallel) = [\langle \mathbf{v}(\mathbf{x}_\parallel + \mathbf{r}_\parallel, t) \cdot \mathbf{v}(\mathbf{x}_\parallel, t)\rangle_\mathbf{x} - \langle \mathbf{v}\rangle_\mathbf{x}^2]/(\langle \mathbf{v}^2\rangle_\mathbf{x} - \langle \mathbf{v}\rangle_\mathbf{x}^2)$ as a function of in-plane distance, and averaged over orientations of $\mathbf{r}_\parallel$ to find $I(r_\parallel)$ as a function of the magnitude $r_\parallel$, and the temporal correlation $J(t) = [\langle \mathbf{v}(\mathbf{x}_\parallel, s + t) \cdot \mathbf{v}(\mathbf{x}_\parallel, s)\rangle_s - \langle \mathbf{v}\rangle_s^2]/(\langle \mathbf{v}^2\rangle_s - \langle \mathbf{v}\rangle_s^2)$. Figure 5(a) shows the first for a pendant drop, averaged over 500 images (16.7 s), along with several of the correlations from pairs of frames. The latter display quite pronounced oscillations reflecting the particular positions of the vortices. The average is of course much smoother but clearly shows anticorrelation extending out to $\sim$100 μm, thus defining the typical scale of a vortex. The associated decay of the temporal correlation in Fig. 5(b) shows that the vortical regions maintain coherence only for a few seconds, the "natural" time scale $\tau = \langle$domain size$\rangle/\langle$domain speed$\rangle$. This scale may reflect the "run-and-tumble" behavior sometimes prevalent in nutrient-depleted suspensions [1]. The average correlation in Fig. 5(b) implies that a collectively generated directional surge is followed by a return flow, and the two particular cases demonstrate vortex street generation. Clearly, these oscillations of the fluid are not inertial, but driven and maintained *by its inhabitants*. The surge and associated shear organizes the gyres, and *their* shear field in turn recruits the local organisms into rotating, internally driven transient domains. While our focus here is on visualization of bacterial swimming patterns, we have also found that micron-size tracers display greatly enhanced diffusion and even superdiffusive behavior over a range of time scales [21], as seen also in bacteria confined to a soap film [22]. Our demonstration of transient, large-scale vortices offers a

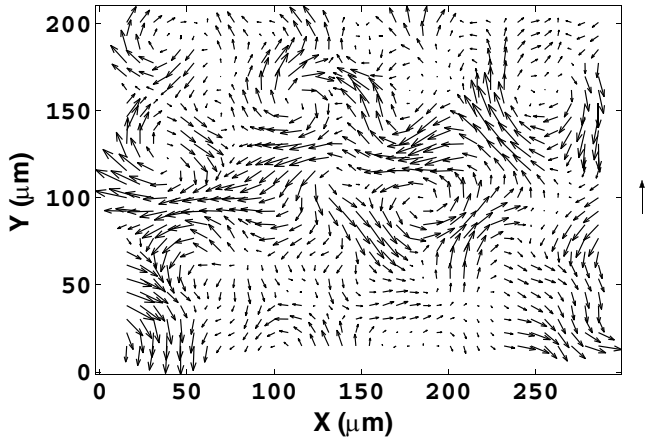

FIG. 4. Flows at the bottom of a pendant drop. Instantaneous bacterial swimming vector field. The arrow at right denotes a speed of 35 μm/s.

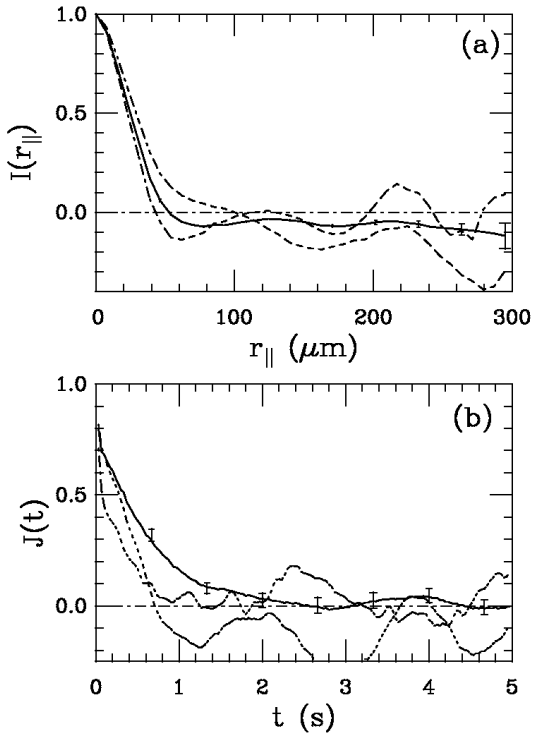

FIG. 5. Correlation functions in a pendant drop: (a) average spatial correlation $I(r)$ (solid) along with several traces at particular times; (b) Average temporal correlation $J(t)$ (solid) with two particular traces.

likely origin for enhanced diffusion: lengthy circulation in the vortical regions followed by "ballistic" motion between them, as seen in rotating fluid layers with persistent vortices [23]. We find that the effective passive tracer (microsphere) diffusion constant can be as large as 10^{-5}–10^{-4} cm^2/s, which can be understood from the processes of trapping and release from these large vortices, since $D_{\text{eff}} \sim \langle \text{domain size} \rangle^2 / \langle \text{lifetime} \rangle \sim 10^{-4}$ cm^2/s

A quantitative theory of the large-scale coherence, intermittency, and high collective velocities requires a novel theoretical synthesis; here we conjecture some key ingredients. The large regions of parallel swimming are indeed reminiscent of flocking, some continuum models of which [3–5] include local nonlinearities in a Navier-Stokes dynamics for the swimming velocity to capture the tendency toward parallel motion. These predict the existence of true long-range swimming order, with parallelism extending to infinity. While we see coherent structures on large scales, they have a *finite* size and limited temporal duration. One mechanism for the disruption of long-range order is suggested from sedimentation, where intermittent, large-scale coherent regions are well known [24]. Their origin is *nonlocal* hydrodynamic interactions which make nearby spheres settle faster than those in isolation. Thus, a fluctuation increasing the local concentration leads to a jet descending faster than its surroundings, which entrains nearby fluid to produce paired, oppositely signed vortices. An analogous effect should occur in swimming suspensions because nearby parallel cells swim faster than those misaligned or in isolation since they are advected by each others' flow fields as their motors output constant power. In more dilute suspensions we observe numerous examples of nearby pairs of cells swimming markedly faster than an individual [25]. This is perhaps not unrelated to the recent proposal for an intrinsic instability of ordered suspensions [6]. It is also possible that the finite depth of the accumulation layer may also play a role in determining the vortical domain size.

There are also implications for the dynamics of intercellular signaling and quorum sensing [8], by which bacteria sense their collective concentration by secreted and detected chemicals. Typical models of chemotactic pattern formation rely on the Keller-Segel model [26], in which diffusion, consumption, and chemotaxis compete, but fluid flow is ignored. Our results show that in the concentrated regime the temporal evolution must include an advective component, the fluid velocity determined self-consistently with the density. Finally, we also find that bacteria become lodged in the narrow wedge-shaped region at the edge of the water, air, solid contact. Initial accumulations of few cells often act to trap many more, suggesting the nucleation of a biofilm, a dense multicellular structure of bacteria and secreted polymers [9]. This experimental setup may provide a useful setting to study in detail the triggering and growth of such films.

We are grateful to D. Coombs, K. Glasner, J. Lega, A. I. Pesci, T. Squires, and K. Visscher for helpful discussions. This work was supported in part by NSF Grant No. MCB0210854.

[1] H. C. Berg, *Random Walks in Biology* (Princeton University Press, Princeton, NJ, 1983).
[2] H. C. Berg and E. M. Purcell, Biophys. J. **20**, 193 (1977).
[3] J. Toner and Y. Tu, Phys. Rev. Lett. **75**, 4326 (1995).
[4] T. Vicsek *et al.*, Phys. Rev. Lett. **75**, 1226 (1995).
[5] A. Czirok, A.-L. Barabási, and T. Vicsek, Phys. Rev. Lett. **82**, 209 (1999).
[6] R. A. Simha and S. Ramaswamy, Phys. Rev. Lett. **89**, 058101 (2002).
[7] Y. Hatwalne, S. Ramaswamy, M. Rao, and R. A. Simha, Phys. Rev. Lett. **92**, 118101 (2004).
[8] B. L. Bassler, Cell **109**, 421 (2002).
[9] G. O'Toole, H. B. Kaplan, and R. Kolter, Annu. Rev. Microbiol. **54**, 49 (2000).
[10] J. O. Kessler and M. F. Wojciechowski, in *Bacteria as Multicellular Organisms*, edited byJ. A. Shapiro and M. Dworkin (Oxford University Press, New York, 1997), p. 417.
[11] R. D. Deegan *et al.*, Nature (London) **389**, 827 (1997).
[12] A *B. subtilis* cell occupies approximately 1 μm^3, so a volume fraction of 1% corresponds to $n \sim 10^{10}$ cm^{-3}.
[13] M. C. Cross and P. C. Hohenberg, Rev. Mod. Phys. **65**, 851 (1993).
[14] N. H. Mendelson and J. Lega, J. Bacteriol. **180**, 3285 (1998).
[15] A. J. Hillesdon, T. J. Pedley, and J. O. Kessler, Bull. Math. Biol. **57**, 299 (1995).
[16] M. Ungarish, *Hydrodynamics of Suspensions* (Springer-Verlag, Berlin, 1993).
[17] D. K. Lubensky and R. E. Goldstein, Phys. Fluids **8**, 843 (1996).
[18] K. Glasner *et al.* (to be published).
[19] C. Dombrowski *et al.* (to be published).
[20] Somewhat similar patterns appear on agar substrates; N. H. Mendelson, *et al.*, J. Bacteriol. **181**, 600 (1999).
[21] J. O. Kessler, in *Proceedings of the International Conference on Differential Equations*, edited by B. Fiedler, K. Gröger, and J. Sprekels (World Scientific, Singapore, 2000), Vol. 2, p. 1284.
[22] X.-L. Wu and A. Libchaber, Phys. Rev. Lett. **84**, 3017 (2000).
[23] T. H. Solomon, E. R. Weeks, and H. L. Swinney, Phys. Rev. Lett. **71**, 3975 (1993).
[24] P. N. Segre, E. Herbolzheimer, and P. M. Chaikin, Phys. Rev. Lett. **79**, 2574 (1997).
[25] J. O. Kessler *et al.*, in *Proceedings of the Workshop on Traffic and Granular Flow '97*, edited by M. Schreckenberg and lf (Springer-Verlag, Singapore, 1998), p. 37.
[26] E. F. Keller and L. A. Segel, J. Theor. Biol. **30**, 225 (1971).